

# Effect of higher-order interactions on noisy majority-rule dynamics with random group sizes

Roni Muslim<sup>1,2,\*</sup>, Jong-Min Park<sup>1,3,†</sup>, Jihye Kim<sup>4,‡</sup> and Rinto Anugraha NQZ<sup>5,§</sup>

<sup>1</sup>*Asia Pacific Center for Theoretical Physics, Pohang, 37673, Republic of Korea*

<sup>2</sup>*Research Center for Quantum Physics, BRIN, South Tangerang, 15314, Indonesia*

<sup>3</sup>*Department of Physics, POSTECH, Pohang 37673, Republic of Korea*

<sup>4</sup>*Department of Physics, Korea University, Seoul, 02841, Republic of Korea and*

<sup>5</sup>*Department of Physics, Universitas Gadjah Mada, Yogyakarta, 55282, Indonesia*

(Dated: February 3, 2026)

We study noisy majority-rule dynamics on annealed hypergraphs to clarify how variability in group interaction sizes reshapes collective ordering. At each update, a group is sampled from a prescribed size distribution and either follows the strict within-group majority or, with probability  $q$ , updates independently under an external bias  $p$ . At the symmetric point  $p = 1/2$ , we obtain an explicit analytical expression for the critical independence threshold  $q_c$ , which separates macroscopic ordering from a fluctuating mixed state and can be interpreted as the largest fraction of independent behavior that can be sustained without destroying order. Because  $q_c$  is governed by group-size statistics through an effective majority leverage, broad and heavy-tailed size distributions enhance robustness by enabling rare large-group events to realign a substantial fraction of the population. We further derive analytical predictions, benchmarked against Monte Carlo simulations, for the leading finite-size behavior of relaxation: for narrow distributions the characteristic relaxation time typically grows logarithmically with system size, whereas sufficiently heavy-tailed power laws produce strong crossovers and make the large-system dynamics sensitive to how  $q$  approaches the transition. In the pure majority-rule limit, we find a crossover from conventional logarithmic consensus times to rapid ordering driven by occasional macroscopic groups, and the exit probability near coexistence collapses onto a universal error-function form controlled by a single structural parameter.

## I. INTRODUCTION

Binary-state opinion models provide a minimal yet powerful framework for probing nonequilibrium collective phenomena in interacting-agent systems [1–3]. Among them, majority-rule (MR) dynamics, also known as the Galam majority rule, serves as a canonical baseline for consensus formation [4–8]. In this model, a set of agents simultaneously adopts its local majority opinion at each update. The rule captures the tension between deterministic alignment induced by local majorities and finite-size stochasticity due to random sampling, thereby shaping macroscopic ordering and relaxation [9–13]. In well-mixed populations, MR yields transparent, analytically tractable predictions for collective outcomes and characteristic time scales, making it a standard reference for social alignment processes and a natural point of departure for higher-order generalizations [14–16]. To quantify these time scales throughout the paper, we use two first-passage observables: the mean consensus time  $T_{\text{cons}}$ , defined as the mean time to reach an absorbing consensus configuration in which all agents share the same state, and the disordering time  $T_{\text{dis}}$ , defined as the mean time for an initially ordered configuration to lose macroscopic order and enter the neighborhood of the stable mixed (disordered) state when such a state exists.

A salient empirical regularity of social interaction is its polyadic nature: deliberation and decision-making typically occur in groups rather than dyads. Hypergraphs and simplicial complexes provide explicit combinatorial representations of such higher-order contacts and have revealed qualitatively new dynamical regimes across contagion and synchronization, including discontinuous social contagion and explosive or abrupt transitions [17–25]. Empirical face-to-face datasets further document group interactions and heterogeneous meeting sizes, underscoring the need for higher-order formalisms [26–31]. Mechanistically related conformity–independence update rules have also been used in agent-based models of green-innovation [32, 33], albeit in a different application context from the noisy hypergraph MR dynamics studied here. In the MR setting, formulating updates on hypergraphs links microscopic group votes to mesoscopic drift-diffusion descriptions; for fixed group sizes (e.g., triplets), diffusion closures reproduce simulations with high fidelity and clarify how group sampling and higher-order structure bias ordering pathways [21, 34–36]. These developments establish hypergraph MR as a principled platform for analyzing collective alignment in multi-person forums and motivate extending the framework to heterogeneous group-size distributions.

The same framework admits a concrete social reading. Hyperedges represent recurrent arenas of discussion, families, committees, work teams, or group-messaging threads, while the hyperedge-size distribution  $P(n)$  encodes heterogeneity in forum sizes, from small huddles to large meetings, as documented in empirical face-to-face and online interaction datasets [26–31]. An “an-

\* contact: roni.muslim@apctp.org

† contact: jongmin.park@apctp.org

‡ contact: arrr3755@naver.com

§ contact: rinto@ugm.ac.id

nealed” representation captures rapidly reconfigured contexts (e.g., rotating committees or fluid online threads), whereas a “quenched” representation reflects persistent group memberships; both are standard coarse-graining choices in nonequilibrium dynamics on networks and higher-order structures [17, 36–38]. In either view, sampling rules and the prevalence of particular group sizes modulate exposure to majority cues, the stability of local agreements, and the pathways to population-level consensus, in line with established insights on group-size effects, classic conformity experiments, and higher-order social contagion [20, 34, 39–41].

Randomness in decision making constitutes a second key ingredient. In the majority-vote (MV) family, a noise parameter competes with local alignment and drives order-disorder transitions whose thresholds and critical properties depend on topology and heterogeneity [42–44]. Socially, such randomness can represent individual autonomy, private information, limited attention, or exogenous messaging that induces updates decoupled from peer influence; a global bias  $p$  plays the role of a directional information field (e.g., institutional guidance or media campaigns), while the independence level  $q$  quantifies the propensity to act irrespective of local pressure. Although MV provides a canonical benchmark for noise-driven symmetry breaking in opinion dynamics, the coupling of independence-type randomness to higher-order, majority-driven group updates on hypergraphs remains comparatively underexplored, especially beyond fixed group sizes and within frameworks that admit drift-diffusion closures [14–18, 34].

Classical results for MR provide the baseline against which noise and higher-order effects can be assessed: on complete graphs, the mean consensus time  $T_{\text{cons}}$  grows logarithmically with system size, and the exit probability approaches a step function in the thermodynamic limit [7, 8]. These benchmarks clarify what must change once independence is introduced and group sizes are allowed to vary. On higher-order structures with fixed hyperedge size, MR admits a drift-dominated, mean-field description with transport coefficients linked directly to microscopic group updates, in close agreement with simulations [34–36]. What remains lacking, however, is a systematic account of noisy MR on hypergraphs with random hyperedge sizes: how an agent-level independence mechanism interacts with an empirically broad  $P(n)$  to set ordering thresholds  $q_c(P)$ , organize relaxation, and reshape exit probabilities in socially heterogeneous environments [28–31, 40].

To close this gap, we develop a unified formulation of noisy majority rule on hypergraphs in which, at each update, a group size  $n$  is drawn from a prescribed distribution  $P(n)$ ; with probability  $1-q$ , the  $n$  agents conform to their local majority, while with probability  $q$ , they update independently, each adopting state  $+1$  with probability  $p$  and  $-1$  with probability  $1-p$ . Here  $q$  denotes an independence probability, distinct from the  $q$  parameter in the  $q$ -voter model, where a related independence mechanism

has been analyzed in our previous work [45]. We retain the explicit  $P(n)$  dependence throughout and combine a mean-field drift-diffusion perspective with Monte Carlo studies on annealed hypergraph ensembles. This framework links microscopic group sampling and independence to macroscopic observables, e.g., consensus times, disordering times, and exit probabilities, while postponing model-specific technicalities and detailed results to the subsequent sections.

## II. MODEL

We consider a population of  $N$  agents, each holding a binary opinion  $\sigma_i \in \{+1, -1\}$ . Interactions occur through hyperedges whose sizes are random. At each elementary update, we first draw a group size  $n$  from a prescribed hyperedge-size distribution  $P(n)$  supported on  $\{n_{\min}, \dots, n_{\max}\}$  with  $n_{\min} \geq 3$  and  $n_{\max} \leq N$ , and then select  $n$  distinct agents uniformly at random from the population. We adopt an annealed (well-mixed) representation in which a fresh hyperedge is resampled at every update, so that only the distribution  $P(n)$ , rather than a fixed underlying hypergraph, matters. One Monte Carlo step (MCS) comprises  $N$  such elementary updates. Let  $t = 0, 1, 2, \dots$  count the number of elementary updates and define the rescaled Monte Carlo time  $\tau \equiv t/N$ , so that one MCS corresponds to  $\Delta\tau = 1$  (i.e.,  $N$  elementary updates), and each elementary update advances time by  $\delta\tau = 1/N$ . Throughout, first-passage observables are measured in units of  $\tau$  (MCS).

We focus on three canonical families of  $P(n)$ : (i) an  $n$ -uniform case with a fixed hyperedge size  $n \geq 3$ ; (ii) a geometric distribution on  $n \geq 3$ , given by  $P_{\text{geo}}(n) = (1-x)x^{n-3}$  with  $0 < x < 1$ , for which  $\langle n \rangle = 3+x/(1-x)$  and hence  $x = (\langle n \rangle - 3)/(\langle n \rangle - 2)$ ; and (iii) a power law  $P_{\text{pl}}(n) = n^{-\alpha}/Z_\alpha$ , where  $Z_\alpha = \sum_{k=n_{\min}}^{n_{\max}} k^{-\alpha}$  is the normalization constant and  $\alpha > 0$ , inspired by empirical data sets [28, 30, 31]. The truncation  $n_{\max}$  enforces feasibility and can be chosen as  $n_{\max} = N$  or as a sublinear cutoff (e.g.,  $n_{\max} = \lfloor N^\kappa \rfloor$  with  $0 < \kappa \leq 1$ ), depending on the application. We allow both odd and even  $n$ ; for even  $n$ , ties are handled explicitly in the update rule.

The dynamics proceeds via random sequential updates. Given a sampled hyperedge  $\{i_1, \dots, i_n\}$  and its pre-update sum  $\Sigma = \sum_{j=1}^n \sigma_{i_j}$ , the state is updated as follows. With probability  $q$  (independence), each of the  $n$  agents is resampled independently of the local configuration, setting  $\sigma_{i_j} = +1$  with probability  $p$  and  $\sigma_{i_j} = -1$  with probability  $1-p$  for  $j = 1, \dots, n$ . With complementary probability  $1-q$  (majority), all  $n$  agents conform to their local majority:  $\sigma_{i_j} = +1$  if  $\Sigma > 0$ ,  $\sigma_{i_j} = -1$  if  $\Sigma < 0$ , and no change occurs if  $\Sigma = 0$  (tie). For the  $n$ -uniform case  $n = 3$ , the dynamics reduces to the triplet MR setting [46]. An illustration of a single update is shown in Fig. 1.

The model is controlled by two parameters:  $q \in [0, 1]$ , the probability of independence (i.e., the likelihood that

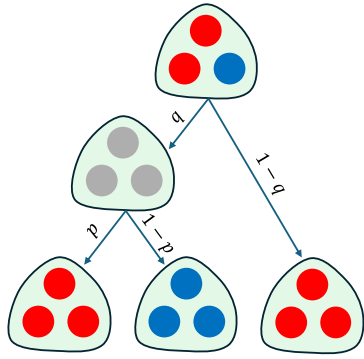


FIG. 1. Schematic illustration of a single update in the model. A hyperedge of size  $n$  (example:  $n = 3$ ) is sampled according to  $P(n)$ , and the within-hyperedge majority state is identified from the pre-update configuration. Each of the  $n$  selected agents then updates as follows: with probability  $1 - q$  it adopts the within-hyperedge majority state, whereas with probability  $q$  it acts independently (ignoring the local majority) and adopts state  $+1$  with probability  $p$  (red) or state  $-1$  with probability  $1 - p$  (blue). Gray nodes indicate the selected agents prior to the update. Ties for even  $n$  yield no change (not shown).

the  $n$  agents update independently of their pre-update configuration), and  $p \in [0, 1]$ , the external bias toward state  $+1$  during independent updates. As the primary macroscopic observable, we track the fraction  $c(\tau)$  of agents holding the  $+1$  opinion. Unless stated otherwise, we consider both balanced initial conditions,  $c(0) = 1/2$ , and fully ordered initial states,  $c(0) \in \{0, 1\}$ , particularly when defining first-passage observables such as consensus times, disordering times, and exit probabilities.

As limiting cases, setting  $q = 0$  recovers the pure majority-rule dynamics on hypergraphs with random group sizes, whereas  $q = 1$  yields fully independent resampling that drives the system toward the fixed point  $c^* = p$  in the thermodynamic limit. The unbiased case  $p = 1/2$  is strictly up-down symmetric (implying no global preference), while  $p \neq 1/2$  represents a directional information field. Throughout this work,  $q$  denotes the independence probability of the present model; it must not be confused with the parameter  $q$  (the size of the lobby group) in the standard  $q$ -voter model, for which a closely related independence mechanism was analyzed in our previous work [45].

### III. TRANSITION PROBABILITIES AND CRITICALITY

#### A. Transition probabilities

The configuration evolves via random sequential updates as described in Sec. II. Let  $c = k/N$  denote the fraction of  $+1$  opinions, where  $k$  is the total number of  $+1$  agents. Since a single hyperedge update may

flip several agents simultaneously, the dynamics constitute a multispin-jump process. Denoting by  $N_{- \rightarrow +}$  and  $N_{+ \rightarrow -}$  the numbers of  $- \rightarrow +$  and  $+ \rightarrow -$  flips produced by one elementary update, the change in  $c$  is  $\Delta c = (N_{- \rightarrow +} - N_{+ \rightarrow -})/N$ . Using the rescaled MC time  $\tau = t/N$  (so that  $\delta\tau = 1/N$  per elementary update), the drift and diffusion coefficients in the diffusion approximation are defined by

$$v(c) = \frac{\langle \Delta c \rangle}{\delta\tau} = N \langle \Delta c \rangle, \quad (1)$$

$$D(c) = \frac{\langle (\Delta c)^2 \rangle - \langle \Delta c \rangle^2}{\delta\tau} = N \text{Var}[\Delta c], \quad (2)$$

where  $\langle \cdot \rangle$  denotes an average over the hyperedge selection and the dynamical noise, and  $\text{Var}[\Delta c]$  is the variance of the one-step increment  $\Delta c$  conditioned on the current state  $c$ .

It is convenient to express these moments in terms of the expected numbers of upward and downward flips per update, defined respectively as  $R(c) \equiv \langle N_{- \rightarrow +} \mid c \rangle$  and  $L(c) \equiv \langle N_{+ \rightarrow -} \mid c \rangle$ . Introducing  $\Delta N \equiv N_{- \rightarrow +} - N_{+ \rightarrow -}$ , Eqs. (1) and (2) can be rewritten as

$$v(c) = R(c) - L(c), \quad (3)$$

$$D(c) = \frac{1}{N} [\langle (\Delta N)^2 \rangle - \langle \Delta N \rangle^2] \quad (4)$$

In the annealed mean-field setting, at each elementary update, a group size  $n$  is drawn from  $P(n)$ , followed by either a majority update with probability  $1 - q$  or an independent update with probability  $q$ . This yields

$$R(c) = \sum_{n=3}^{n_{\max}} P(n) \left[ (1 - q) M_n(c) + q n p (1 - c) \right], \quad (5)$$

$$L(c) = \sum_{n=3}^{n_{\max}} P(n) \left[ (1 - q) M_n(1 - c) + q n (1 - p) c \right], \quad (6)$$

where  $M_n(c) = \sum_{\ell=\lfloor n/2 \rfloor + 1}^n (n - \ell) \binom{n}{\ell} c^\ell (1 - c)^{n - \ell}$  is the expected number of  $- \rightarrow +$  flips generated by a strict majority of  $+1$  opinions in a group of size  $n$  (ties produce no flips), while  $M_n(1 - c)$  gives the corresponding  $+ \rightarrow -$  flips under a strict majority of  $-1$ . The independence contributions in Eqs. (5)–(6) arise because, on average, a fraction  $1 - c$  (respectively,  $c$ ) of the sampled hyperedge is in state  $-1$  (respectively,  $+1$ ), and each such agent adopts state  $+1$  with probability  $p$  and state  $-1$  with probability  $1 - p$ .

Substituting Eqs. (5)–(6) into Eq. (3) yields the explicit drift

$$v(c) = \sum_{n=3}^{n_{\max}} P(n) \{ (1 - q) \Delta M_n(c) + q n (p - c) \}, \quad (7)$$

where  $\Delta M_n(c) \equiv M_n(c) - M_n(1 - c)$ . The second term in braces is the independence contribution that drives

the system toward the externally preferred value  $c = p$ , while the first term represents the restoring tendency of the strict majority rule. Both contributions are averaged over the hyperedge-size distribution  $P(n)$ . The onset of ordering is determined by the linear stability of the disordered fixed point; specifically, for  $p = 1/2$  (so that  $c_{\text{dis}} = 1/2$ ), the critical value  $q_c$  follows from the condition  $v'(1/2) = 0$ . For later use, we also record the explicit form of the second jump moment  $S(c) \equiv \langle (\Delta N)^2 \rangle$ . Conditioned on a fixed group size  $n$ , one has

$$S(c) = \sum_{n=3}^{n_{\max}} P(n) \left[ (1-q) S_n^{\text{MR}}(c) + q S_n^{\text{ind}}(c) \right], \quad (8)$$

and the diffusion coefficient then follows exactly from Eq. (4) as  $D(c) = S(c)/N - v(c)^2/N$ . The majority-rule contribution to the second moment is

$$S_n^{\text{MR}}(c) = \sum_{\ell=\lfloor \frac{n}{2} \rfloor + 1}^n (n-\ell)^2 B_{n,\ell}(c) + \sum_{\ell=0}^{\lfloor \frac{n-1}{2} \rfloor} \ell^2 B_{n,\ell}(c), \quad (9)$$

where  $B_{n,\ell}(c) = \binom{n}{\ell} c^\ell (1-c)^{n-\ell}$ . For the independent update, letting  $\ell$  be the number of +1 agents before the update and  $\ell'$  after the update, one has  $\ell \sim \text{Bin}(n, c)$  and  $\ell' \sim \text{Bin}(n, p)$  (independent), hence  $\Delta N = \ell' - \ell$  and

$$\begin{aligned} S_n^{\text{ind}}(c) &= \langle (\ell' - \ell)^2 \rangle \\ &= n p (1-p) + n c (1-c) + n^2 (p-c)^2. \end{aligned} \quad (10)$$

Averaging Eqs. (9)–(10) over  $P(n)$  yields  $S(c)$ , and inserting into Eq. (4) gives the full diffusion coefficient  $D(c)$  governing stochastic fluctuations in the FP description.

## B. Criticality

At the up-down symmetric point  $p = 1/2$ , the balanced state  $c = 1/2$  is always a fixed point. The order–disorder transition occurs when this fixed point changes its linear stability.

Using the drift in Eq. (7) and the antisymmetry  $\Delta M_n(1-c) = -\Delta M_n(c)$ , we expand  $v(c)$  around the fixed point  $c = 1/2$ . To leading order in the deviation  $\delta c = c - 1/2$  (see Appendix A), one obtains the linearized form

$$v(c) \simeq [(1-q) \mathcal{A}_1(P) - q \langle n \rangle] (c - 1/2), \quad (11)$$

where  $\langle n \rangle = \sum_n n P(n)$  is the mean hyperedge size, and  $\mathcal{A}_1(P)$  measures the average strength of the majority rule near the symmetric point. This coefficient is given by

$$\mathcal{A}_1(P) = \sum_{n=3}^{n_{\max}} P(n) 2^{2-n} S_n, \quad (12)$$

where the combinatorial factor  $S_n = \sum_{\ell=\lfloor n/2 \rfloor + 1}^n (n-\ell)(2\ell-n)\binom{n}{\ell}$  represents the specific majority leverage for

groups of size  $n$ . Physically, the first term in the bracket of Eq. (11) describes the ordering tendency driven by majority-rule updates, while the term proportional to  $q \langle n \rangle$  reflects the tendency of independent updates to relax the system toward the unbiased state  $c = 1/2$ . Equivalently,  $\mathcal{A}_1(P)$  quantifies how strongly a majority update amplifies small imbalances away from  $c = 1/2$ , whereas  $q \langle n \rangle$  quantifies how strongly independence suppresses such imbalances by re-randomizing agents within the selected hyperedge.

The disordered fixed point  $c = 1/2$  loses stability when the slope  $v'(1/2)$  becomes positive (i.e., when the drift pushes the system away from 1/2). Setting the term in square brackets in Eq. (11) to zero yields the critical independence level

$$q_c(P) = \frac{\mathcal{A}_1(P)}{\mathcal{A}_1(P) + \langle n \rangle}. \quad (13)$$

This expression highlights that  $q_c(P)$  is determined by the competition between the average majority leverage  $\mathcal{A}_1(P)$  and the independence-induced relaxation  $\langle n \rangle$ . Physically,  $q_c(P)$  sets the independence level at which the linear stability of the symmetric mixed state changes: for  $q < q_c(P)$  majority amplification dominates and the symmetric mixed state is unstable, whereas for  $q > q_c(P)$  independent updates dominate and stabilize the mixed state around  $c = 1/2$ . Hence, an increase in  $q_c$  means that ordering is more robust against independence noise, i.e., a stronger independent tendency is required to destroy macroscopic order.

Specializing Eq. (13) to the three hyperedge-size families yields explicit expressions for the critical independence level. For the  $n$ -uniform ensemble, we have

$$q_c(n) = \frac{2^{2-n} S_n}{2^{2-n} S_n + n}. \quad (14)$$

For the geometric distribution, the summation leads to

$$q_c(x) = \frac{(1-x)^2 \sum_{n=3}^{\infty} x^{n-3} 2^{2-n} S_n}{(1-x)^2 \sum_{n=3}^{\infty} x^{n-3} 2^{2-n} S_n + (3-2x)}. \quad (15)$$

In this case, the threshold  $q_c$  is an increasing function of the mean group size  $\langle n \rangle = (3-2x)/(1-x)$ , indicating that larger interaction groups enhance majority amplification and therefore require a larger independence probability to destroy order.

For the truncated power-law ensemble, the normalization constants cancel in Eq. (13), yielding

$$q_c(\alpha) = \frac{\sum_{n=3}^N n^{-\alpha} 2^{2-n} S_n}{\sum_{n=3}^N n^{-\alpha} 2^{2-n} S_n + \sum_{n=3}^N n^{1-\alpha}}. \quad (16)$$

In the thermodynamic limit  $N \rightarrow \infty$ , this expression converges to

$$q_c(\alpha) \rightarrow \begin{cases} 1, & \alpha \leq 5/2, \\ \frac{\sum_{n=3}^{\infty} n^{-\alpha} 2^{2-n} S_n}{\sum_{n=3}^{\infty} n^{-\alpha} 2^{2-n} S_n + \zeta(\alpha-1, 3)}, & \alpha > 5/2, \end{cases} \quad (17)$$

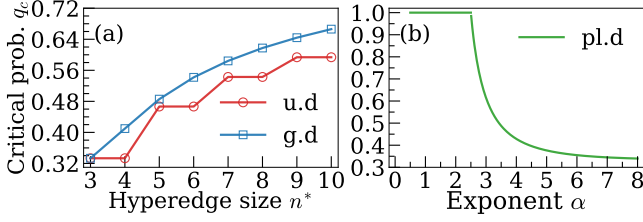


FIG. 2. Phase diagram of the noisy majority-rule dynamics on annealed hypergraphs in the up-down symmetric case  $p = 1/2$ . (a)  $q_c$  for the  $n$ -uniform ensemble [Eq. (14)] and the shifted geometric ensemble [Eq. (15)], plotted versus the characteristic group size  $n^* \equiv n = \langle n \rangle$ . (b)  $q_c(\alpha)$  for the truncated power-law ensemble as a function of the tail exponent  $\alpha$  [Eq. (17)]. The ordered phase corresponds to  $q < q_c$ , while the disordered phase corresponds to  $q > q_c$ .

where  $\zeta(a, b)$  denotes the Hurwitz zeta function. Thus, a genuine order-disorder transition exists only for  $\alpha > 5/2$ . In this regime,  $q_c(\alpha)$  decreases monotonically with  $\alpha$  and approaches  $q_c = 1/3$  as  $\alpha \rightarrow \infty$ , where the distribution becomes effectively 3-uniform. Conversely, for  $\alpha \leq 5/2$ , the system remains ordered for any  $q < 1$ . Equivalently, in the thermodynamic limit the mixed state becomes linearly stable only in the fully independent limit  $q \rightarrow 1$ .

Equations (14)–(17) show how higher-order interaction patterns control the tolerance of ordering to independence noise through  $q_c$ . In particular, distributions biased toward larger group sizes increase the majority leverage  $\mathcal{A}_1(P)$ , so a larger independence probability is required to stabilize the mixed state, yielding a larger  $q_c$  [Fig. 2(a)]. For truncated power-law ensembles, small exponents  $\alpha$  place substantial weight on large hyperedges, driving  $q_c(\alpha)$  toward unity, whereas for large  $\alpha$  the distribution is dominated by small groups and  $q_c$  approaches the  $n = 3$  limit,  $q_c \rightarrow 1/3$ . In this sense, heavy-tailed  $P(n)$  makes disordering harder: rare but large hyperedges produce strong majority amplification, so the system can remain ordered even when independent behavior is frequent.

#### IV. CONSENSUS TIME

##### A. Pure majority-rule regime

The consensus time or ordering time is the mean first-passage time (MFPT) for the coarse-grained fraction  $c(\tau)$  of  $+1$  opinions to reach an absorbing consensus configuration, i.e.,  $c = 1$  (all agents in state  $+1$ ) or  $c = 0$  (all agents in state  $-1$ ), starting from a partially ordered initial condition. In the pure majority-rule dynamics ( $q = 0$ ), updates are governed solely by the local majority within the sampled hyperedge, so the characteristic time scale is controlled by the hyperedge size or its distribution  $P(n)$ . In the thermodynamic limit, the fixed point at  $c = 1/2$  is linearly unstable; trajectories with  $c(0) > 1/2$  flow to

$c = 1$ , whereas those with  $c(0) < 1/2$  flow to  $c = 0$ . Dynamically, consensus is drift-dominated away from the separatrix at  $c = 1/2$ , while demographic fluctuations set the width of the initial neighborhood from which the system escapes, leading to the characteristic logarithmic growth of the MFPT with  $N$  in well-mixed settings.

A standard analysis employs the backward Kolmogorov description for the one-dimensional process  $c(\tau)$  with drift  $v(c)$  and diffusion  $D(c)$ . The MFPT from  $c_0$  to an absorbing boundary  $c_b$  (assuming a reflecting boundary at  $c_a$ ; e.g.,  $c_a = 1/2$ ,  $c_b = 1 - 1/N$ ) solves  $v(c)T'(c) + \frac{1}{2}D(c)T''(c) = -1$  with  $T'(c_a) = 0$  and  $T(c_b) = 0$ . The solution is given by the quadrature [47, 48]

$$T(c_0) = \int_{c_0}^{c_b} dy \exp(-\Psi(y)) \int_{c_a}^y dx \frac{2 \exp(\Psi(x))}{D(x)}, \quad (18)$$

where  $\Psi(c) = \int_{c_a}^c [2v(z)/D(z)] dz$ . All dependence on the higher-order structure enters through  $v(c)$  and  $D(c)$ , which are determined by the majority leverage of size- $n$  groups averaged over  $P(n)$ .

The quadrature in Eq. (18) does not admit a closed form for general  $P(n)$ . However, in the large- $N$  (drift-dominated) regime, the Wentzel–Kramers–Brillouin limit applies: the exponential kernels localize, and the MFPT is dominated by the deterministic time of flight of the coarse-grained dynamics  $dc/d\tau = v(c)$ :

$$T \approx \int_{c_i}^{c_f} \frac{dc}{v(c)}. \quad (19)$$

Here,  $c_i$  and  $c_f$  are chosen along a deterministic trajectory so that  $v(c)$  has the same sign as  $(c_f - c_i)$ , ensuring  $T > 0$ . Physically, Eq. (19) implies that in well-mixed populations, majority-induced drift sets the ordering pace, whereas demographic fluctuations merely fix the width of the initial boundary layer the system must escape.

For initially balanced configurations, we regularize the unstable fixed point at  $c = 1/2$  by displacing the initial condition by its natural finite-size fluctuation,  $c_i = 1/2 + \delta$  with  $\delta \sim N^{-1/2}$ , and we set the absorbing threshold at  $c_f = 1 - 1/N$ . The shift  $\delta$  reflects the typical demographic imbalance arising from random initial conditions, representing the minimal bias that majority pressure can amplify [48]. The choice  $c_f = 1 - 1/N$  avoids the singular boundary at  $c = 1$  while capturing the “last minority” conversion. This prescription prevents long, uninformative sojourns near the unstable point and isolates the genuine  $N$ -dependence of the consensus time.

Evaluating the integral in Eq. (19) yields the robust scaling

$$T_{\text{cons}} \sim \mathcal{B} \ln N, \quad (20)$$

with a prefactor  $\mathcal{B}$  that has a clear physical interpretation. The logarithm arises from two stages: (i) the escape from the vicinity of the unstable state ( $c \simeq 1/2$ ), and (ii)

the approach to full consensus where the remaining minority is swept out. The first stage is determined by the local slope of the majority drift near  $c = 1/2$ , while the second is controlled by the typical group size near the absorbing boundary.

Specializing to the annealed  $n$ -uniform ensemble, the two contributions combine into the prefactor (see Appendix B)

$$\mathcal{B}(n) = \frac{1}{n} + \frac{2^{n-3}}{S_n}, \quad (21)$$

where  $S_n$  quantifies the net restoring effect of strict majorities in size- $n$  groups. Equation (21) holds for both odd and even  $n$ : for even  $n$ , tie events correspond to  $\ell = n/2$  and are excluded by construction in  $S_n$ , yielding no flips. The term  $1/n$  reflects the final elimination of the last minority, whereas the term  $2^{n-3}/S_n$  accounts for the slow passage through the nearly balanced region.

For a geometric hyperedge-size distribution with parameter  $x$ , the prefactor becomes

$$\mathcal{B}(x) = \frac{1-x}{3-2x} + \frac{1}{\sum_{n \geq 3} (1-x)x^{n-3} 2^{3-n} S_n}. \quad (22)$$

Here, the first term corresponds to  $1/\langle n \rangle$  (final sweep), while the second measures the inverse of the effective majority leverage near  $c \simeq 1/2$ .

For a truncated power law with cutoff  $n_{\max} = N$ , the finite- $N$  prefactor reads

$$\mathcal{B}(N, \alpha) = \frac{\sum_{n=3}^N n^{-\alpha}}{\sum_{n=3}^N n^{1-\alpha}} + \frac{\sum_{n=3}^N n^{-\alpha}}{\sum_{n=3}^N n^{-\alpha} 2^{3-n} S_n}. \quad (23)$$

In the thermodynamic limit, the asymptotic behavior depends on  $\alpha$ :

$$\mathcal{B}(\alpha) = \begin{cases} 0, & \alpha \leq 2, \\ \frac{\zeta(\alpha, 3)}{\zeta(\alpha - 1, 3)}, & 2 < \alpha \leq 5/2, \\ \frac{\zeta(\alpha, 3)}{\zeta(\alpha - 1, 3)} + \frac{\zeta(\alpha, 3)}{\sum_{n=3}^{\infty} n^{-\alpha} 2^{3-n} S_n}, & \alpha > 5/2. \end{cases} \quad (24)$$

For  $\alpha \leq 2$ , the prefactor vanishes as  $N \rightarrow \infty$ , signaling that the consensus time grows slower than  $\ln N$  (or saturates). For  $\alpha > 2$ , the prefactor is strictly positive, and  $T_{\text{cons}}$  recovers the logarithmic form  $T_{\text{cons}} \sim \mathcal{B}(\alpha) \ln N$ . Note that for  $2 < \alpha \leq 5/2$ , only the first term in Eq. (23) survives in the limit, while for  $\alpha > 5/2$ , both contributions remain finite.

Equations (22)–(25) reveal a consistent physical trend: shifting  $P(n)$  toward larger group sizes (which typically increases the truncated mean  $\langle n \rangle_N$  and enhances the weight of large- $n$  events) strengthens the effective majority leverage and thus speeds up ordering. For the  $n$ -uniform case,  $\mathcal{B}(n)$  decreases monotonically with  $n$ , yielding the longest consensus time at  $n = 3$  [ $T_{\text{max}}(N) =$

$(2/3) \ln N$ ] and tending to zero as  $n \rightarrow \infty$ . This monotonicity holds for both odd and even  $n$ , since tie events for even  $n$  contribute no flips and are excluded by construction in the strict-majority sums defining  $S_n$ . Similarly, for the geometric distribution,  $\mathcal{B}(x)$  decreases with the mean size  $\langle n \rangle$ . This suggests that larger groups exhibit stronger majority-restoring tendencies, correcting deviations from consensus more efficiently.

The truncated power-law ensemble exhibits the strongest sensitivity to group sizes. Here, varying the exponent  $\alpha$  changes both the tail weight and the truncated mean size  $\langle n \rangle_N(\alpha)$ ; therefore the  $\alpha$ -dependence of  $T_{\text{cons}}$  reflects the combined effect of suppressing/allowing large hyperedges and changing  $\langle n \rangle_N$ . Heavy tails ( $\alpha \leq 2$ ) assign significant weight to very large hyperedges, which can align macroscopic fractions of the system in a single update, causing  $T_{\text{cons}}$  to saturate or grow sublogarithmically. Conversely, for lighter tails ( $\alpha > 2$ ), the relevant moments are finite and the logarithmic scaling holds. As  $\alpha \rightarrow \infty$ , the size distribution becomes effectively 3-uniform, and the prefactor approaches the  $n = 3$  limit,  $\mathcal{B} \rightarrow 2/3$ .

For fixed system size  $N$ , these dependencies are visualized in Fig. 4.  $T_{\text{cons}}$  decreases monotonically with increasing group size (uniform/geometric) and increases with the exponent  $\alpha$  (power law), consistent with the shift of probability weight toward smaller hyperedges and the concomitant decrease of  $\langle n \rangle_N(\alpha)$  for our truncation. The Monte Carlo data [Fig. 4(a)–(c)] closely match these analytical predictions.

When the initial condition is displaced by an  $O(1)$  amount from the unstable fixed point, the dynamical bottleneck at  $c = 1/2$  is bypassed. Consequently, the mean consensus time is determined solely by the final approach to the absorbing boundary. To leading order, one recovers the logarithmic scaling of Eq. (20), but with a prefactor that lacks the contribution from the unstable fixed point. This modified prefactor depends only on the statistics of the hyperedge sizes:

For the annealed  $n$ -uniform distribution, the prefactor simplifies to

$$\mathcal{B}(n) = \frac{1}{n}, \quad (25)$$

indicating that consensus accelerates inversely with group size. For the shifted geometric distribution,

$$\mathcal{B}(x) = \frac{1-x}{3-2x}, \quad (26)$$

which is a decreasing function of the mean size  $\langle n \rangle = (3-2x)/(1-x)$ .

For the truncated power law, with natural cutoff

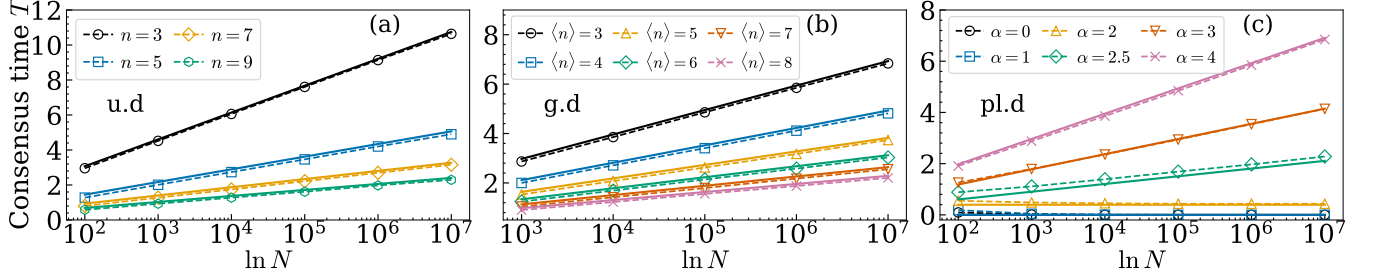


FIG. 3. Consensus time  $T$  versus system size  $N$  for three hyperedge-size distributions starting from the balanced initial condition  $c(0) = 1/2$ : (a) annealed  $n$ -uniform for several  $n$ ; (b) shifted geometric for several mean sizes  $\langle n \rangle$ ; and (c) truncated power law for several tail exponents  $\alpha$ . Solid curves show the mean-field prediction from Eq. (20) with the corresponding prefactors, while symbols connected by dashed lines are MC data averages over  $10^5$  runs. The data confirm the predicted crossover: logarithmic growth with a distribution-dependent prefactor for uniform/geometric ensembles and for power laws with  $\alpha > 2$ , and saturation for heavy tails  $\alpha \leq 2$ .

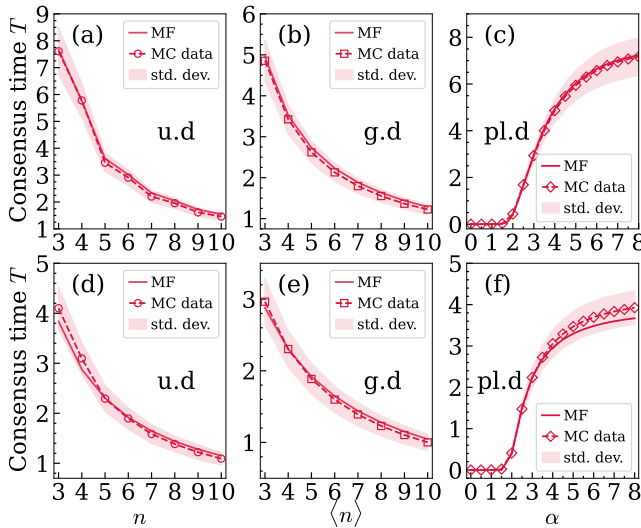


FIG. 4. Consensus time  $T$  at fixed system size  $N = 10^5$  for three hyperedge-size distributions under two initial conditions. Panels (a)–(c): balanced start  $c(0) = 0.5$ . Panels (d)–(f): unbalanced start  $c(0) = 0.7$ . (a),(d) Annealed  $n$ -uniform (varying  $n$ ); (b),(e) shifted geometric (varying  $\langle n \rangle$ ); (c),(f) truncated power law (varying  $\alpha$ ). Solid curves: mean-field predictions. Symbols with dashed lines: MC averages over  $10^5$  realizations. Shaded bands: one standard deviation.

$n_{\max} = N$ , the prefactor exhibits three distinct regimes:

$$\mathcal{B}(N, \alpha) \simeq \begin{cases} 0, & \alpha < 2, \\ \frac{\zeta(2, 3)}{\ln N}, & \alpha = 2, \\ \frac{\zeta(\alpha, 3)}{\zeta(\alpha - 1, 3)}, & \alpha > 2. \end{cases} \quad (27)$$

Thus, genuine logarithmic scaling persists only for  $\alpha > 2$ . At the marginal point  $\alpha = 2$ , the logarithmic growth of  $T_{\text{cons}}$  is canceled by the vanishing prefactor ( $\mathcal{B} \sim 1/\ln N$ ), resulting in an  $N$ -independent saturation. For

$\alpha < 2$ , the consensus time is similarly  $O(1)$ .

These mean-field predictions are confirmed by the simulations in Fig. 4(d)–(f):  $T_{\text{cons}}$  decreases with increasing  $n$  or  $\langle n \rangle$ , and increases with  $\alpha$ . This is consistent with the physical intuition that heavy-tailed distributions (small  $\alpha$ ) facilitate rapid consensus by frequently sampling large, highly efficient groups.

## B. Independence regime

In the regime with independence ( $q > 0$ ), the dynamics interpolates between strict local conformity (probability  $1 - q$ ) and independent resampling biased by the external bias  $p$  (probability  $q$ ), whereby each selected agent adopts state  $+1$  with probability  $p$  and state  $-1$  with probability  $1 - p$ . The nature of the stationary state depends critically on the bias strength  $p$ . For intermediate biases  $0 < p < 1$ , the independence mechanism stabilizes a mixed attractor, preventing absorbing consensus. However, in the limit of extreme bias  $p \in \{0, 1\}$ , the external field breaks the symmetry fully, and the system is driven toward a unique absorbing state. This scenario corresponds to a monolithic information environment (e.g., fully aligned media) that overrides local disagreements and locks the population into a single prevailing opinion [49, 50].

For the extreme-bias cases  $p \in \{0, 1\}$ , the dynamical bottleneck at  $c = 1/2$  vanishes. The consensus time is therefore controlled solely by the relaxation of the boundary layer near the absorbing state. Consequently, the leading asymptotic behavior coincides with that of the pure majority-rule regime starting from unbalanced conditions, recovering the scaling  $T_{\text{cons}} \sim \mathcal{B} \ln N$  with the prefactors given in Eqs. (25)–(27) (see Appendix C for details). The system bypasses the metastable “hung” state and proceeds directly via the progressive erosion of the minority.

Remarkably, in this limit, the logarithmic prefactor  $\mathcal{B}$  becomes independent of the independence level  $q$ . This

universality arises because, at extreme bias, the local majority rule and the directional bias  $p$  act constructively. Near the absorbing boundary (e.g.,  $c \rightarrow 1$  with  $p = 1$ ), a selected hyperedge containing minority agents will convert them to the majority state regardless of whether the update is driven by peer pressure (majority rule) or by the intrinsic bias encoded in  $p$  (independence). Mathematically, the drift in the boundary layer scales as  $v(c) \simeq \langle n \rangle(p - c)$  for both mechanisms, leading to identical relaxation times. This robustness of the consensus time against the independence level  $q$  mirrors analogous findings in our previous work [45].

## V. DISORDERING TIME

We define the disordering time  $T_{\text{dis}}$  as the MFPT required for the system to reach the neighborhood of the disordered state ( $c = 1/2$ ) starting from a fully ordered configuration. This observable is physically meaningful in the up-down symmetric case  $p = 1/2$  within the disordered regime  $q > q_c$ , where the fixed point at  $c = 1/2$  is linearly stable. In this regime,  $T_{\text{dis}}$  quantifies the robustness of consensus against noise: it measures how long an initially ordered population resists erosion under the combined action of local majority updates and independence-driven fluctuations.

As in the consensus-time analysis, we adopt the backward FP picture and apply the drift-dominated approximation. The MFPT corresponds to the deterministic time of flight  $dc/d\tau = v(c)$  integrated from the ordered boundary layer ( $c \approx 1$ ) into the basin of attraction of the stable fixed point  $c = 1/2$ . Based on the linearization in Eq. (11), the drift close to  $c = 1/2$  can be written as  $v(c) \simeq -\lambda(c - 1/2)$  with the relaxation rate  $\lambda = q\langle n \rangle - (1 - q)\mathcal{A}_1$ , which is strictly positive in the disordered phase  $q > q_c$ . The integration is cut off at  $c_f = 1/2 + O(N^{-1/2})$  to reflect the width of stationary fluctuations. This logarithmic approach to the fixed point dominates the integral, yielding the scaling

$$T_{\text{dis}} \sim \mathcal{B} \ln N, \quad (28)$$

with a prefactor  $\mathcal{B} = 1/(2\lambda)$ . Note that  $\mathcal{B}$  diverges as  $q \rightarrow q_c^+$ , signaling the critical slowing down of the relaxation process.

For the annealed  $n$ -uniform ensemble, substituting the explicit rate  $\lambda$  into the prefactor yields (see Appendix D)

$$\mathcal{B}(n, q) = \left[ 2q n - (1 - q) 2^{3-n} S_n \right]^{-1}. \quad (29)$$

Similarly, for the shifted geometric distribution, summing over the group sizes gives

$$\mathcal{B}(x, q) = \left[ 2q \frac{3 - 2x}{1 - x} - (1 - q)(1 - x) \Phi(x) \right]^{-1}, \quad (30)$$

where  $\Phi(x) = \sum_{n=3}^{\infty} x^{n-3} 2^{3-n} S_n$  converges absolutely for  $|x| < 1$ .

For the truncated power-law ensemble, the relaxation rate becomes  $N$ -dependent because the effective majority leverage  $\mathcal{A}_1(P)$  diverges for  $\alpha \leq 5/2$  (cf. Sec. III B). To make this explicit, we write the linear relaxation rate near  $c = 1/2$  as

$$\lambda_N \equiv q \langle n \rangle_N - (1 - q)\mathcal{A}_1(N, \alpha), \quad (31)$$

where  $\langle n \rangle_N$  and  $\mathcal{A}_1(N, \alpha)$  are evaluated with the finite-size cutoff  $n_{\text{max}} = N$ . The drift-dominated estimate then reads

$$T_{\text{dis}}(N; \alpha, q) \sim \frac{\ln N}{2\lambda_N}, \quad (32)$$

provided  $\lambda_N > 0$ , i.e., provided that  $c = 1/2$  is linearly stable at the chosen  $(N, \alpha, q)$ .

The interpretation is as follows. For  $\alpha > 5/2$ , both  $\langle n \rangle_N$  and  $\mathcal{A}_1(N, \alpha)$  converge, so  $\lambda_N \rightarrow \lambda_\infty$  and Eq. (32) yields the genuine logarithmic growth  $T_{\text{dis}} \sim [2\lambda_\infty]^{-1} \ln N$ . For  $\alpha \leq 5/2$ ,  $\mathcal{A}_1(N, \alpha)$  diverges with  $N$ , implying  $q_c(N) \rightarrow 1$  and hence the disordered regime requires  $q$  to approach 1 as  $N$  increases; at fixed absolute  $q < 1$ , the fixed point  $c = 1/2$  remains unstable asymptotically, and the disordering MFPT (as defined here) is not the appropriate descriptor of the long- $N$  dynamics. In finite systems, one may still observe rapid relaxation toward coexistence for  $q$  sufficiently close to 1, in which case Eq. (32) remains the correct starting point, with  $\lambda_N$  set by the finite-size cutoff.

A useful consistency check is the extreme independence limit  $q = 1$ , where majority updates are absent. In this case,  $\lambda = \langle n \rangle$  and the prefactor reduces to  $\mathcal{B} = 1/(2\langle n \rangle)$ . This implies that disordering proceeds twice as fast (i.e., with half the time prefactor) as consensus formation from unbalanced initial conditions in the pure majority-rule regime [cf. Eqs. (25)–(27)]. For instance, for the shifted geometric distribution, one recovers  $\mathcal{B}(1, x) = (1 - x)/[2(3 - 2x)]$ . The factor of two originates from the different finite-size cutoffs: approaching an absorbing boundary requires reducing the minority to  $O(1)$  agents (a distance  $\sim 1/N$ ), whereas approaching the stable coexistence fixed point only requires reaching the scale of stationary fluctuations around  $c = 1/2$  (a distance  $\sim N^{-1/2}$ ).

To compare different hyperedge-size distributions on an equal footing, it is convenient to parameterize the distance from criticality as  $q = \kappa q_c$  with  $\kappa > 1$ . This protocol is meaningful whenever  $q_c(P) < 1$  (in particular for the uniform and shifted-geometric ensembles, and for the truncated power-law ensemble with  $\alpha > 5/2$  in the thermodynamic limit). This guarantees that the system is in the disordered phase regardless of the specific  $P(n)$ . Substituting  $q = \kappa q_c$  into the linear relaxation rate  $\lambda$  and using the definition of  $q_c$  yields  $\lambda = (\kappa - 1)\mathcal{A}_1(P)$ . Consequently, the disordering time obeys the compact scaling

form

$$T_{\text{dis}}(N, \kappa) \sim \frac{\ln N}{2(\kappa - 1)\mathcal{A}_1(P)}. \quad (33)$$

The parameter  $\kappa$  controls the proximity to the threshold: as  $\kappa \rightarrow 1^+$ , the system exhibits critical slowing down with divergence  $(\kappa - 1)^{-1}$ . The factor  $\mathcal{A}_1(P)$  quantifies the structural stability provided by the hypergraphs. At a fixed relative distance  $\kappa$ , a larger  $\mathcal{A}_1(P)$  implies a larger critical threshold  $q_c$ , and hence a larger absolute independence level  $q = \kappa q_c$ , leading to faster relaxation toward coexistence. The scaling form Eq. (33) is well supported by MC data for all three families of  $P(n)$  as shown in Fig. 5.

For the  $n$ -uniform and shifted-geometric ensembles,  $T_{\text{dis}}$  decreases as the characteristic group size increases. This trend follows from the increase of  $q_c$  with group size; consequently, at fixed  $\kappa$ , the corresponding absolute noise level  $q = \kappa q_c$  is larger, leading to faster relaxation toward the disordered state.

For power-law ensembles, the same intuition must be qualified because the effective moments of  $P(n)$  may depend on  $N$  under the cutoff, and the outcome becomes protocol dependent. At fixed absolute  $q$ , heavy tails lead to vanishing disordering times as  $N \rightarrow \infty$  because the mean size  $\langle n \rangle$  diverges and the independence component dominates the dynamics. At fixed relative distance  $\kappa$  above threshold,  $T_{\text{dis}}$  increases with  $\alpha$  (see Fig. 6). In this constant- $\kappa$  comparison, lighter tails (large  $\alpha$ ) imply smaller average group sizes and weaker majority leverage  $\mathcal{A}_1(P)$ , thereby slowing down the relaxation toward disorder.

## VI. EXIT PROBABILITY

A central observable in opinion dynamics is the exit probability  $E(c_0)$ , defined as the probability that the dynamics reaches the all-+1 absorbing state ( $c = 1$ ) before the all-−1 state ( $c = 0$ ), starting from an initial fraction  $c(0) = c_0$  of +1 agents. In the diffusion approximation for the coarse-grained density  $c(\tau)$ ,  $E(c)$  satisfies the backward FP boundary-value problem

$$v(c) E'(c) + \frac{1}{2} D(c) E''(c) = 0, \quad (34)$$

with absorbing boundary conditions  $E(0) = 0$  and  $E(1) = 1$ .

In the pure majority-rule regime ( $q = 0$ ), the dynamics is symmetric under spin reversal, making  $c = 1/2$  a fixed point. Following a standard saddle-point treatment of the backward FP problem near the symmetric point (see Appendix E), one obtains an explicit scaling form for  $E(c_0)$ . The new element in the present setting is that the higher-order interaction structure enters this scaling form through a single parameter  $\gamma(P)$ , and we provide  $\gamma(P)$  explicitly for the ensembles considered. In the central scaling regime, the exit probability takes a universal

error-function form:

$$E(c_0) \approx \frac{1}{2} \left[ 1 + \text{erf} \left( \sqrt{\gamma(P)} \left( c_0 - \frac{1}{2} \right) \right) \right], \quad (35)$$

where  $\gamma(P) = \mathcal{A}_1(P)/D_0(P)$ . Here,  $\mathcal{A}_1(P)$  is the average majority leverage defined in Eq. (12), and  $D_0(P) \equiv D(1/2)$  is the diffusion coefficient evaluated at the symmetric point. The explicit expressions for specific ensembles are provided in Eqs. (E6)–(E8) of Appendix E. Equation (35) shows that, within the diffusion description, different higher-order structures are distinguished solely by  $\gamma(P)$ , which measures the ratio between majority amplification and stochastic fluctuations near the separatrix  $c = 1/2$ .

The diffusion approximation underlying Eq. (35) assumes that the elementary increments  $\Delta c$  are small, so that truncating the KM expansion at second order is accurate. This assumption holds well for the uniform and shifted-geometric ensembles, where hyperedge sizes are bounded or decay exponentially. For heavy-tailed power-law ensembles, however, sufficiently small exponents allow occasional hyperedges with  $n = O(N)$ , which induce macroscopic jumps in  $c$  and violate the small-jump assumption. In that regime, the standard FP description tends to underestimate the steepness of the exit-probability curve. Accordingly, we use Eq. (35) as a scaling baseline and expect quantitative agreement primarily in parameter ranges where large- $n$  events are sufficiently suppressed (see Appendix E for details). A fully quantitative theory for strongly heavy-tailed cases would require the discrete master equation with nonlocal transitions, which is beyond the scope of the present work.

Nevertheless, Eq. (35) provides a robust scaling framework when the diffusion approximation applies. To make finite-size effects explicit, it is convenient to introduce the scaling variable  $z = \sqrt{\gamma(P)} (c_0 - \frac{1}{2})$ . In terms of  $z$ , Eq. (35) reads  $E(c_0) \approx \frac{1}{2} [1 + \text{erf}(z)]$ , so that all dependence on  $N$  and on the hyperedge-size statistics is absorbed into the rescaling of the initial condition. Plotting  $E$  as a function of  $z$  collapses the data for different system sizes (at fixed  $P$ ) onto a single universal curve, as illustrated in the inset of Fig. 7.

From the definition of  $\gamma(P)$ , the width of the transition region scales as  $\Delta c \sim \gamma(P)^{-1/2} \propto \sqrt{D_0/\mathcal{A}_1}$ . Since  $D_0 \sim N^{-1}$  while  $\mathcal{A}_1$  is  $O(1)$ , we recover the standard mean-field finite-size scaling  $\Delta c \sim N^{-1/2}$ . Thus, for large but finite  $N$ , Eq. (35) quantifies how  $P(n)$  controls the sharpness of the probabilistic crossover near  $c_0 = 1/2$  through  $\gamma(P)$ , while in the thermodynamic limit the curve sharpens into a step function.

## VII. SUMMARY AND CONCLUSION

We have investigated a noisy majority-rule dynamics on annealed hypergraphs in which, at each update, a group of size  $n$  is drawn from a prescribed distribution  $P(n)$ . In this framework, selected agents either conform

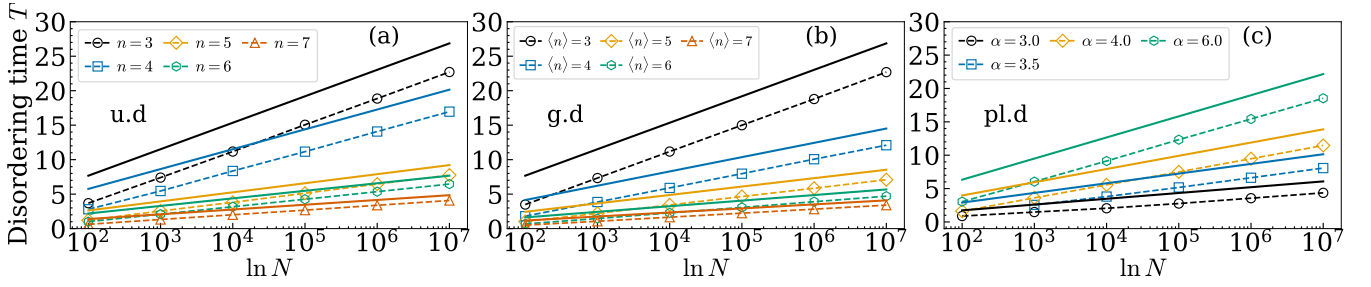


FIG. 5. Disordering time  $T_{\text{dis}}$  versus system size  $N$  for three hyperedge-size distributions starting from the fully ordered state  $c(0) = 1$ : (a) annealed  $n$ -uniform for various  $n$ ; (b) shifted geometric for various  $\langle n \rangle$ ; (c) truncated power law for various  $\alpha$ . Data are shown at a fixed relative distance from the threshold,  $q = \kappa q_c$  with  $\kappa = 1.2$ . Solid curves: mean-field prediction of Eq. (33) with the corresponding prefactors. Symbols with dashed lines: MC averages over  $10^5$  runs. The data confirm the logarithmic growth in the disordered phase ( $q > q_c$ ) for all distributions, including power laws with  $\alpha > 5/2$ .

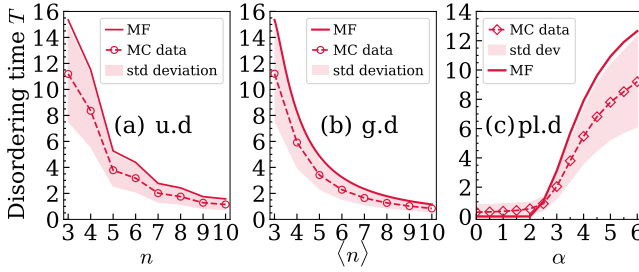


FIG. 6. Disordering time  $T_{\text{dis}}$  as a function of system size  $N$  at a fixed distance from criticality,  $\kappa = 1.2$ . Panels show (a)  $n$ -uniform, (b) shifted geometric, and (c) truncated power law. Solid lines are mean-field predictions from Eq. (33), while dashed lines with symbols are MC results; shaded regions indicate one standard deviation. For the truncated power-law ensemble, varying  $\alpha$  changes both the tail weight and the truncated mean size  $\langle n \rangle_N(\alpha)$  (for fixed cutoffs), so the observed  $\alpha$  dependence reflects the combined effect of suppressing large- $n$  events and reducing  $\langle n \rangle_N$ . The data confirm that at fixed  $\kappa$ , systems with smaller effective group sizes (small  $n$ , small  $\langle n \rangle$ , or larger  $\alpha$ , which shifts probability weight toward smaller hyperedges and lowers  $\langle n \rangle_N$ ) relax more slowly.

to the strict local majority (with probability  $1 - q$ ) or update independently according to an external bias  $p$  (with probability  $q$ ). Our main goal was to isolate how fluctuations in interaction-group size, encoded by  $P(n)$ , reshape ordering, disordering, and finite-size relaxation beyond the fixed- $n$  baseline.

At the up-down symmetric point  $p = 1/2$ , the model exhibits an order-disorder transition controlled by the independence probability  $q$ . By performing a Landau-like expansion of the drift around the mixed fixed point, we derived a general expression for the critical independence level  $q_c(P)$  in terms of the mean group size and a structural coefficient quantifying the average majority leverage. Analytical predictions for  $n$ -uniform, shifted geometric, and truncated power-law ensembles agree well with MC simulations. Physically,  $q_c(P)$  quantifies the maximal fraction of independent updates that the sys-

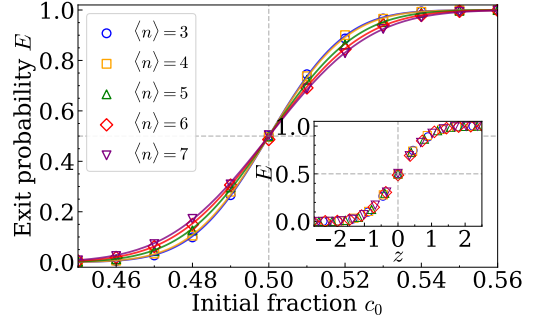


FIG. 7. Exit probability  $E$  versus initial fraction  $c_0$  for the shifted geometric distribution with various mean hyperedge sizes  $\langle n \rangle$  ( $N = 10^3$ ). Main panel: Comparison between MC simulations (symbols) and the diffusion-theory prediction from Eq. (35) (solid lines). Inset: Data collapse obtained by plotting  $E$  against the scaling variable  $z = \sqrt{\gamma}(c_0 - 1/2)$ .

tem can tolerate while still sustaining macroscopic order; broader distributions that place more weight on large groups increase this tolerance by amplifying majority alignment. For  $n$ -uniform and geometric distributions,  $q_c$  increases with the characteristic group size. For power-law ensembles,  $q_c(\alpha)$  approaches the triplet limit  $1/3$  as  $\alpha \rightarrow \infty$ , whereas heavy-tailed statistics (small  $\alpha$ ) assign significant weight to large hyperedges, pushing  $q_c$  toward unity.

In the disordered phase  $q > q_c(P)$ , we characterized the disordering time  $T_{\text{dis}}$ , defined as the mean time to reach the vicinity of the mixed state starting from a fully ordered configuration. Combining a diffusion approximation with a backward FP treatment, we obtained a logarithmic system-size dependence  $T_{\text{dis}} \sim \mathcal{B}(P, q) \ln N$  for large system sizes. For  $n$ -uniform and geometric ensembles, the prefactor remains finite for all  $q > q_c$ , ensuring logarithmic growth. However, for truncated power-law ensembles, the dynamics depends sharply on the tail exponent: the logarithmic scaling persists only for  $\alpha > 5/2$ . For heavy tails with  $\alpha \leq 5/2$ , the divergent fluctuations of the hyperedge size accelerate relaxation, caus-

ing  $T_{\text{dis}}$  to become  $O(1)$  (i.e., to no longer grow with  $N$ ) in the large- $N$  limit under the natural cutoff. In the limit of extreme bias ( $p \in \{0, 1\}$ ), where consensus becomes absorbing, the consensus time  $T_{\text{cons}}$  exhibits the same distribution-controlled size dependence as the corresponding relaxation time in the unbiased setting, highlighting the central role of  $P(n)$  in setting ordering time scales.

In the pure majority-rule regime ( $q = 0$ ), we analyzed the exit probability  $E(c_0)$ , the likelihood of reaching the all- $+1$  state from an initial fraction  $c_0$ . We showed that, near the symmetric point,  $E(c_0)$  collapses onto a universal error-function profile governed by a single scaling variable that combines  $c_0$ , the system size  $N$ , and the hyperedge statistics. Ensembles that emphasize larger groups possess a higher ratio of drift to diffusion, effectively sharpening the transition and making small initial advantages deterministically decisive. Conversely, ensembles dominated by small groups broaden the transition region, enhancing the role of stochasticity. For sufficiently heavy-tailed ensembles, occasional macroscopic jumps can limit the quantitative accuracy of the diffusion description, although the scaling framework still captures the qualitative sharpening mechanism.

In summary, our results show that the full group-size distribution  $P(n)$  controls (i) the robustness of ordering through  $q_c(P)$  and (ii) the characteristic relaxation time scales, including crossovers induced by rare large-group events. Natural extensions of this work include the study of quenched hypergraphs, the interplay between higher-order and pairwise interactions, and the effects of time-dependent or competing external fields. These directions would help connect distribution-controlled higher-order ordering mechanisms to empirically grounded group-interaction data in social and technological systems.

## ACKNOWLEDGMENTS

**R. Muslim** was supported by the YST Program of the Asia Pacific Center for Theoretical Physics (APCTP), funded by the Science and Technology Promotion Fund and Lottery Fund of the Korean Government, and by the Management Talent Program of the National Research and Innovation Agency of Indonesia (BRIN). **J.-M. Park** acknowledges support from an appointment to the JRG Program at APCTP through the Science and Technology Promotion Fund and Lottery Fund of the Korean Government. This work was also supported by the Korean Local Governments—Gyeongsangbuk-do Province and Pohang City. This work was supported by the National Research Foundation of Korea (NRF) grant funded by the Korea government (MSIT) (Grant No. RS-2025-00557038).

## Appendix A: Rate Equations and Criticality

We consider the noisy majority-rule (MR) dynamics with independent updates introduced in Sec. II. The configuration evolves via random sequential elementary updates. In each update, a group (hyperedge) of size  $n \geq 3$  is drawn from the prescribed size distribution  $P(n)$  and  $n$  distinct agents are selected uniformly at random. With probability  $q$  (independence), each selected agent is resampled independently, taking  $+1$  with probability  $p$  and  $-1$  with probability  $1 - p$ . With probability  $1 - q$  (majority rule), all selected agents adopt the within-group majority opinion; for even  $n$ , tie events ( $\Sigma = 0$ ) yield no change. Throughout, we measure time in Monte Carlo steps (MCS) using the rescaled variable  $\tau = t/N$ , where  $t$  counts elementary updates, so that  $\delta\tau = 1/N$  per update.

Let  $R(c) \equiv \langle N_{-\rightarrow+} \mid c \rangle$  and  $L(c) \equiv \langle N_{+\rightarrow-} \mid c \rangle$  denote the conditional expectations of the numbers of  $-1 \rightarrow +1$  and  $+1 \rightarrow -1$  flips produced by a single elementary update, given the current density  $c$  of  $+1$  opinions. In the annealed mean-field setting, these rates read

$$R(c) = \sum_{n \geq 3} P(n) [(1 - q) M_n(c) + q n p (1 - c)],$$

$$L(c) = \sum_{n \geq 3} P(n) [(1 - q) M_n(1 - c) + q n (1 - p) c], \quad (\text{A1})$$

where  $M_n(c) = \sum_{\ell=\lfloor n/2 \rfloor+1}^n (n - \ell) \binom{n}{\ell} c^\ell (1 - c)^{n - \ell}$  is the expected number of  $-1 \rightarrow +1$  flips generated by a majority update in a size- $n$  group when a strict  $+1$  majority is present (for even  $n$ , ties do not contribute). The complementary term  $M_n(1 - c)$  accounts for strict  $-1$  majorities.

Accordingly, the coarse-grained drift per unit  $\tau$  is

$$v(c) \equiv \frac{\langle \Delta c \rangle}{\delta\tau} = R(c) - L(c)$$

$$= \sum_{n \geq 3} P(n) \left\{ q n (p - c) + (1 - q) \Delta M_n(c) \right\}, \quad (\text{A2})$$

with  $\Delta M_n(c) \equiv M_n(c) - M_n(1 - c)$ . Solving the stationarity condition  $v(c) = 0$  for  $q$  at arbitrary  $c$  yields

$$q(c) = \frac{\sum_{n \geq 3} P(n) \Delta M_n(c)}{\sum_{n \geq 3} P(n) \Delta M_n(c) + (c - p) \langle n \rangle}, \quad (\text{A3})$$

where  $\langle n \rangle \equiv \sum_{n \geq 3} n P(n)$ .

For the up-down symmetric case  $p = 1/2$ , the disordered state  $c = 1/2$  is always a fixed point. To analyze the order-disorder transition, we perform a linear expansion of the drift around this critical point. Let  $c = 1/2 + \delta$ , where  $|\delta| \ll 1$ .

Expanding the binomial probability weight  $B_{n,\ell}(c) \equiv \binom{n}{\ell} c^\ell (1 - c)^{n - \ell}$  to first order in  $\delta$  yields

$$B_{n,\ell}(1/2 + \delta) = \binom{n}{\ell} (1/2 + \delta)^\ell (1/2 - \delta)^{n - \ell}$$

$$\simeq 2^{-n} \binom{n}{\ell} [1 + 2(2\ell - n)\delta]. \quad (\text{A4})$$

Substituting this into the majority-rule drift term  $\Delta M_n(c) = M_n(c) - M_n(1 - c)$  and using the antisymmetry around  $c = 1/2$ , we obtain

$$\begin{aligned}\Delta M_n(c) &\simeq \sum_{\ell=\lfloor \frac{n}{2} \rfloor + 1}^n (n - \ell) [B_{n,\ell}(1/2 + \delta) - B_{n,\ell}(1/2 - \delta)] \\ &= \sum_{\ell=\lfloor \frac{n}{2} \rfloor + 1}^n (n - \ell) \binom{n}{\ell} 2^{-n} [4(2\ell - n)\delta] \\ &= 2^{2-n} S_n (c - 1/2),\end{aligned}\quad (\text{A5})$$

where  $S_n = \sum_{\ell=\lfloor n/2 \rfloor + 1}^n (n - \ell) (2\ell - n) \binom{n}{\ell}$ .

Finally, the critical independence probability is obtained from the condition  $v'(c)|_{c=1/2} = 0$ . The derivative of the total drift [Eq. (A2)] with respect to  $c$  at  $c = 1/2$  is

$$v'(1/2) = (1 - q) \sum_{n \geq 3} P(n) 2^{2-n} S_n - q \langle n \rangle. \quad (\text{A6})$$

Setting  $v'(1/2) = 0$  yields the critical threshold as

$$\begin{aligned}q_c &= \frac{\sum_{n \geq 3} P(n) 2^{2-n} S_n}{\sum_{n \geq 3} P(n) 2^{2-n} S_n + \langle n \rangle} \\ &= \frac{\mathcal{A}_1(P)}{\mathcal{A}_1(P) + \langle n \rangle},\end{aligned}\quad (\text{A7})$$

where  $\mathcal{A}_1(P) \equiv \sum_{n \geq 3} P(n) 2^{2-n} S_n$  is the mean majority leverage.

## 1. Annealed $n$ -uniform distribution

For the  $n$ -uniform ensemble with fixed group size  $n$ , the distribution is given by  $P(k) = \delta_{k,n}$ . Substituting this into Eq. (A7), the sums collapse to single terms:

$$q_c(n) = \frac{S_n}{S_n + n 2^{n-2}}, \quad (\text{A8})$$

which coincides with Eq. (14) in the main text.

## 2. Geometric distribution

Consider the truncated (shifted) geometric distribution on  $n \geq 3$ ,

$$P(n) = \frac{(1 - x)x^{n-3}}{1 - x^{N-2}}, \quad 0 < x < 1, \quad (\text{A9})$$

where the denominator ensures  $\sum_{n=3}^N P(n) = 1$ , which corresponds to the parameterization  $x = (\langle n \rangle - 3)/(\langle n \rangle -$

2) in the thermodynamic limit. The truncated mean is

$$\begin{aligned}\langle n \rangle &= \sum_{n=3}^N n P(n) \\ &= \frac{(1 - x)}{1 - x^{N-2}} \sum_{j=0}^{N-3} (j + 3) x^j \\ &= 3 + \frac{x[1 - (N - 2)x^{N-3} + (N - 3)x^{N-2}]}{(1 - x^{N-2})(1 - x)}.\end{aligned}\quad (\text{A10})$$

In the limit  $N \rightarrow \infty$ , the term  $x^{N-2} \rightarrow 0$ , yielding the standard result

$$\langle n \rangle = \frac{3 - 2x}{1 - x}. \quad (\text{A11})$$

Moreover, the weighted sum in the numerator becomes

$$\begin{aligned}\sum_{n=3}^N P(n) 2^{2-n} S_n &= \frac{1 - x}{1 - x^{N-2}} \sum_{n=3}^N x^{n-3} 2^{2-n} S_n \\ &= (1 - x) \sum_{n=3}^{\infty} x^{n-3} 2^{2-n} S_n.\end{aligned}\quad (\text{A12})$$

Inserting Eqs. (A11)–(A12) into Eq. (A7) yields the asymptotic critical point

$$q_c(x) = \frac{(1 - x) \sum_{n=3}^{\infty} x^{n-3} 2^{2-n} S_n}{(1 - x) \sum_{n=3}^{\infty} x^{n-3} 2^{2-n} S_n + \frac{3 - 2x}{1 - x}}, \quad (\text{A13})$$

which coincides with Eq. (15) in the main text.

## 3. Power-law distribution

For the truncated power-law ensemble, we consider  $P(n) = n^{-\alpha}/Z_\alpha$  with  $Z_\alpha = \sum_{n=3}^N n^{-\alpha}$  and  $\alpha > 0$ . Note that varying  $\alpha$  changes not only the tail weight, but also the truncated mean hyperedge size

$$\langle n \rangle_N(\alpha) \equiv \sum_{n=3}^N n P(n) = \frac{\sum_{n=3}^N n^{1-\alpha}}{\sum_{n=3}^N n^{-\alpha}} = \frac{B_N(\alpha)}{Z_\alpha}, \quad (\text{A14})$$

which will be useful when interpreting  $\alpha$ -dependent trends. Returning to Eq. (A7), it is convenient to rewrite the finite- $N$  critical point as

$$q_c(\alpha; N) = \frac{A_N(\alpha)}{A_N(\alpha) + B_N(\alpha)}, \quad (\text{A15})$$

where  $A_N(\alpha) \equiv \sum_{n=3}^N n^{-\alpha} 2^{2-n} S_n$  and  $B_N(\alpha) \equiv \sum_{n=3}^N n^{1-\alpha}$ . In Eq. (A15),  $B_N(\alpha)$  is directly proportional to the first moment of the size distribution (cf. Eq. (A14)), while  $A_N(\alpha)$  encodes the majority-amplification factor  $2^{2-n} S_n$  and therefore depends on the full distribution of group sizes, not only on  $\langle n \rangle_N$ .

To estimate  $A_N(\alpha)$  for large  $n$ , we use a Gaussian approximation for the binomial coefficient,

$$\binom{n}{\ell} \approx 2^n \sqrt{\frac{2}{\pi n}} \exp \left[ -\frac{2(\ell - n/2)^2}{n} \right]. \quad (\text{A16})$$

Writing  $\ell = n/2 + j$  and approximating the sum by an integral, one obtains the leading asymptotic behavior

$$2^{2-n} S_n \sim n^{3/2} \quad (n \gg 1). \quad (\text{A17})$$

Substituting this into the definition of  $A_N(\alpha)$ , we find

$$A_N(\alpha) \sim \sum_{n=3}^N n^{3/2-\alpha}. \quad (\text{A18})$$

From Eq. (A18), one finds that  $A_N(\alpha)$  scales as  $N^{5/2-\alpha}$  for  $\alpha < 5/2$ , grows logarithmically as  $\ln N$  for  $\alpha = 5/2$ , and converges to a finite constant  $A(\alpha) = \sum_{n=3}^{\infty} n^{-\alpha} 2^{2-n} S_n$  for  $\alpha > 5/2$ .

For the moment term  $B_N(\alpha) = \sum_{n=3}^N n^{1-\alpha}$ , standard estimates show that  $B_N(\alpha) \propto N^{2-\alpha}$  for  $\alpha < 2$ ,  $B_N(2) \sim \ln N$ , and  $B_N(\alpha) \rightarrow \zeta(\alpha - 1, 3)$  for  $\alpha > 2$ , where  $\zeta(a, b)$  is the Hurwitz zeta function. Consequently, for our truncation  $n_{\max} = N$ , the mean size  $\langle n \rangle_N(\alpha) = B_N(\alpha)/Z_\alpha$  increases as  $\alpha$  decreases and becomes  $N$ -dependent for  $\alpha \leq 2$  (diverging as  $N \rightarrow \infty$ ), reflecting the growing weight of large hyperedges.

Combining these asymptotics in Eq. (A15), we obtain the thermodynamic limit:

$$q_c(\alpha) \equiv \lim_{N \rightarrow \infty} q_c(\alpha; N) = \begin{cases} 1, & \alpha \leq 5/2, \\ \frac{A(\alpha)}{A(\alpha) + \zeta(\alpha - 1, 3)}, & \alpha > 5/2. \end{cases} \quad (\text{A19})$$

Thus, the critical threshold tends to unity for all  $\alpha \leq 5/2$  and converges to a finite value in  $(0, 1)$  for  $\alpha > 5/2$ .

In the limit  $\alpha \rightarrow \infty$ , the distribution concentrates on the smallest hyperedge size,  $P(n) \rightarrow \delta_{n,3}$ . For  $n = 3$ , one has  $S_3 = \sum_{\ell=2}^2 (3-\ell)(2\ell-3) \binom{3}{\ell} = 3$ , so that  $2^{2-3} S_3 = 3/4$  and  $\langle n \rangle = 3$ . Using Eq. (A7) specialized to the  $n = 3$  case, i.e.,  $q_c = (2^{2-3} S_3) / [(2^{2-3} S_3) + \langle n \rangle / 2]$ , we recover the limiting value  $q_c(\infty) = (3/4)/(3/4 + 3/2) = 1/3$ .

## Appendix B: Consensus Time

### 1. Pure majority-rule dynamics with an initially balanced state

In the mean-field limit, the diffusion term is negligible since  $D(c) = \mathcal{O}(1/N)$ . The consensus time is obtained by integrating the inverse drift characteristic  $d\tau = dc/v(c)$  from the backward Kolmogorov equation:

$$T \approx \int_{c_f}^{c_i} -\frac{dc}{v(c)}. \quad (\text{B1})$$

The integration bounds are determined by the microscopic fluctuation widths: the initial state is taken just outside the unstable fixed point,  $c_i = 1/2 - N^{-1/2}$ , and the final state is at the absorption scale,  $c_f = 1/N$ .

The integral in Eq. (B1) is dominated by the divergences near the two fixed points  $c = 0$  and  $c = 1/2$ . We can therefore approximate the total time as the sum of the transit times across these two bottlenecks:

$$T \approx T_{\text{abs}} + T_{\text{cen}}. \quad (\text{B2})$$

For a general hyperedge size distribution  $P(n)$ , the drift linearizes near these fixed points as follows:

*Near the absorbing boundary ( $c \rightarrow 0$ ):* The minority opinion vanishes linearly with a rate determined by the mean group size  $\langle n \rangle$ . The drift is  $v(c) \simeq -\langle n \rangle c$ , yielding the contribution

$$T_{\text{abs}} \approx \int_{1/N}^{\text{const}} \frac{dc}{\langle n \rangle c} = \frac{1}{\langle n \rangle} \ln N. \quad (\text{B3})$$

*Near the central fixed point ( $c \rightarrow 1/2$ ):* The drift is linear in the deviation,  $v(c) \simeq \mathcal{A}_1(P)(c - 1/2)$ . Integrating from the fluctuation scale yields

$$T_{\text{cen}} \approx \int_{\text{const}}^{\frac{1}{2} - \frac{1}{\sqrt{N}}} -\frac{dc}{\mathcal{A}_1(P)(c - 1/2)} \approx \frac{1}{2\mathcal{A}_1(P)} \ln N. \quad (\text{B4})$$

Combining these, the general scaling for the consensus time is

$$T(N) \sim \left[ \frac{1}{\langle n \rangle} + \frac{1}{2\mathcal{A}_1(P)} \right] \ln N. \quad (\text{B5})$$

We now evaluate the specific coefficients  $\langle n \rangle$  and  $\mathcal{A}_1(P)$  for the different ensembles.

#### a. Annealed $n$ -uniform distribution

For the  $n$ -uniform ensemble, the coefficients are simply  $\langle n \rangle = n$ , and  $\mathcal{A}_1(n) = 2^{2-n} S_n$ . Substituting these into Eq. (B5) immediately yields

$$T(n, N) \sim \left[ \frac{1}{n} + \frac{2^{n-3}}{S_n} \right] \ln N, \quad (\text{B6})$$

recovering Eq. (21) in the main text.

#### b. Geometric distribution

For the truncated geometric distribution, the mean size corresponds to the effective rate at the boundary,  $\langle n \rangle = (3 - 2x)/(1 - x)$ . The leverage term corresponds to the rate at the center, with the asymptotic limit for  $\mathcal{A}_1(P)$  given by Eq. (A12). Substituting these coefficients into the general expression Eq. (B5) yields

$$T(N, x) \sim \left[ \frac{1-x}{3-2x} + \frac{1}{2(1-x) \sum_{n \geq 3} x^{n-3} 2^{2-n} S_n} \right] \ln N, \quad (\text{B7})$$

which matches Eq. (22) in the main text.

### c. Power-law distribution

We consider an annealed power-law ensemble where hyperedge sizes  $n \in \{3, \dots, N\}$  are drawn from

$$P_N(n) = \frac{n^{-\alpha}}{Z_N(\alpha)}, \quad Z_N(\alpha) = \sum_{n=3}^N n^{-\alpha}, \quad (\text{B8})$$

with exponent  $\alpha > 0$ . To apply the general consensus time formula derived in Eq. (B5), we identify the relevant macroscopic rates. The inverse boundary rate is determined by the first moment sum  $B_N$ , and the inverse central repulsion rate is determined by the majority leverage sum  $C_N$ :

$$\langle n \rangle = \frac{B_N(N, \alpha)}{Z_N(\alpha)}, \quad \text{with} \quad B_N = \sum_{n=3}^N n^{1-\alpha}, \quad (\text{B9})$$

$$2\mathcal{A}_1(P) = \frac{C_N(N, \alpha)}{Z_N(\alpha)}, \quad \text{with} \quad C_N = \sum_{n=3}^N n^{-\alpha} 2^{3-n} S_n. \quad (\text{B10})$$

Substituting these into Eq. (B5) yields the prefactor

$$T(N, \alpha) \sim \left[ \frac{Z_N(\alpha)}{B_N(N, \alpha)} + \frac{Z_N(\alpha)}{C_N(N, \alpha)} \right] \ln N. \quad (\text{B11})$$

To analyze the thermodynamic limit, we determine the asymptotic behavior of the three sums. The normalization  $Z_N(\alpha)$  and the first moment  $B_N(N, \alpha)$  follow standard power-law sum rules:

$$Z_N \sim \begin{cases} \frac{N^{1-\alpha}}{1-\alpha}, & \alpha < 1, \\ \ln N, & \alpha = 1, \\ \zeta(\alpha, 3), & \alpha > 1, \end{cases} \quad B_N \sim \begin{cases} \frac{N^{2-\alpha}}{2-\alpha}, & \alpha < 2, \\ \ln N, & \alpha = 2, \\ \zeta(\alpha-1, 3), & \alpha > 2. \end{cases} \quad (\text{B12})$$

For the majority leverage sum  $C_N(N, \alpha)$ , recalling that  $S_n \sim n^{3/2} 2^{n-3}$  for large  $n$ , the summand scales as  $n^{-\alpha} 2^{3-n} (n^{3/2} 2^{n-3}) \sim n^{3/2-\alpha}$ . This implies a divergence threshold at  $\alpha = 5/2$ :

$$C_N(\alpha) \sim \begin{cases} N^{\frac{5}{2}-\alpha}, & \alpha < \frac{5}{2}, \\ \ln N, & \alpha = \frac{5}{2}, \\ C_N^{(\infty)}(\alpha), & \alpha > \frac{5}{2}, \end{cases} \quad (\text{B13})$$

where  $C_N^{(\infty)}(\alpha) = \sum_{n=3}^{\infty} n^{-\alpha} 2^{3-n} S_n$  is a convergent constant.

Based on these asymptotics, we identify three distinct scaling regimes for the consensus time prefactor  $\mathcal{B}(\alpha)$ :

1. Regime  $0 < \alpha \leq 2$ : The boundary term  $Z_N/B_N$  vanishes as  $N \rightarrow \infty$  (scaling as  $N^{-1}$  for  $\alpha < 1$ ,  $N^{\alpha-2}$  for  $1 < \alpha < 2$ , and  $(\ln N)^{-1}$  for  $\alpha = 2$ ). Since  $C_N$  diverges even faster than  $B_N$ , the central term  $Z_N/C_N$  also vanishes. Thus,  $\mathcal{B}(\alpha) \rightarrow 0$ , meaning the consensus time grows slower than logarithmic (or saturates).

2. Regime  $2 < \alpha \leq 5/2$ : The sums  $Z_N$  and  $B_N$  converge to finite Riemann zeta values, but  $C_N$  continues to diverge (or grows logarithmically at  $\alpha = 5/2$ ). Consequently, the central contribution  $Z_N/C_N$  vanishes. The dynamics is dominated solely by the transit time near the absorbing boundary:

$$\mathcal{B}(\alpha) = \frac{\zeta(\alpha, 3)}{\zeta(\alpha-1, 3)}. \quad (\text{B14})$$

3. Regime  $\alpha > 5/2$ : All three sums converge. Both the absorbing boundary and the unstable central point contribute to the time scale. The prefactor becomes the sum of both characteristic times:

$$\mathcal{B}(\alpha) = \frac{\zeta(\alpha, 3)}{\zeta(\alpha-1, 3)} + \frac{\zeta(\alpha, 3)}{A_2^{(\infty)}(\alpha)}. \quad (\text{B15})$$

Summarizing these results, the consensus time prefactor  $\mathcal{B}(\alpha)$  is given by

$$\mathcal{B}(\alpha) = \begin{cases} 0, & \alpha \leq 2, \\ \frac{\zeta(\alpha, 3)}{\zeta(\alpha-1, 3)}, & 2 < \alpha \leq \frac{5}{2}, \\ \frac{\zeta(\alpha, 3)}{\zeta(\alpha-1, 3)} + \frac{\zeta(\alpha, 3)}{\sum_{n=3}^{\infty} n^{-\alpha} 2^{3-n} S_n}, & \alpha > \frac{5}{2}, \end{cases} \quad (\text{B16})$$

consistent with Eq. (24) in the main text.

## Appendix C: Consensus time with independence

For  $q > 0$  under extreme bias  $p \in \{0, 1\}$ , the fully ordered states become absorbing ( $c = 1$  for  $p = 1$  and  $c = 0$  for  $p = 0$ ). In this regime, the drift  $v(c)$  remains non-zero at  $c = 1/2$ , eliminating the dynamical bottleneck associated with the unstable fixed point. Consequently, the consensus time is determined solely by the relaxation dynamics within the boundary layer near the absorbing state.

For initial conditions bounded away from the separatrix (i.e., fixed  $c(0) \neq 1/2$  as  $N \rightarrow \infty$ ), the dynamics is drift-dominated. In the boundary layer, the drift scales linearly as  $v(c) \simeq \langle n \rangle (1-c)$  for  $p = 1$  (and symmetrically  $v(c) \simeq -\langle n \rangle c$  for  $p = 0$ ), where  $\langle n \rangle = \sum_n n P(n)$ . This linear relaxation implies that the leading asymptotic behavior of the consensus time is identical to that of the pure majority-rule dynamics ( $q = 0$ ) starting from an unbalanced initial state.

## Appendix D: Disordering Time

In the disordered phase  $q > q_c$ , the mixed state  $c = 1/2$  is linearly stable. For large  $N$ , the diffusion term is subleading, so the entrance into the disordered basin is

governed by the drift  $v(c)$ . Linearizing  $v(c)$  at  $p = 1/2$  around  $c = 1/2$  yields

$$\begin{aligned} v(c) &\simeq v'(1/2)(c - 1/2) \\ &= -\frac{1}{2} \left[ q\langle n \rangle - (1-q)\mathcal{A}_1(P) \right] (2c - 1). \end{aligned} \quad (\text{D1})$$

For an initial condition fixed away from  $c = 1/2$ , integrating down to the fluctuation boundary  $c_f = 1/2 + 1/\sqrt{N}$  gives

$$\begin{aligned} T(N, q, P) &\approx \int_1^{1/2+N^{-1/2}} \frac{dc}{v(c)} \\ &\sim \frac{\ln N}{2[q\langle n \rangle - (1-q)\mathcal{A}_1(P)]}. \end{aligned} \quad (\text{D2})$$

To parametrize distances from criticality, write  $q = \kappa q_c$  with  $\kappa > 1$ . Substituting  $q_c$  from Eq. (A7) into the denominator of Eq. (D2) simplifies the term in the brackets to  $(\kappa - 1)\mathcal{A}_1(P)$ . Consequently, Eq. (D2) becomes

$$T(N, \kappa) \sim \frac{\ln N}{2(\kappa - 1)\mathcal{A}_1(P)}, \quad (\text{D3})$$

showing that  $T$  scales linearly with  $\ln N$  and diverges as  $(\kappa - 1)^{-1}$  near criticality.

### 1. Annealed $n$ -uniform distribution

For the annealed  $n$ -uniform ensemble one has  $\langle n \rangle = n$  and  $\mathcal{A}_1(n) = 2^{2-n}S_n$ . Substituting into Eq. (D2) gives

$$T(N, q, n) \sim \frac{\ln N}{2[qn - (1-q)2^{2-n}S_n]}, \quad (\text{D4})$$

in agreement with Eq. (29) in the main text. Equivalently, the disordering time can be written as

$$T(N, \kappa) \sim \frac{\ln N}{2(\kappa - 1)\mathcal{A}_1(n)} = \frac{2^{n-3}}{(\kappa - 1)S_n} \ln N. \quad (\text{D5})$$

### 2. Annealed geometric distribution

For the annealed geometric distribution, substituting  $\langle n \rangle$  and  $\mathcal{A}(x)$  from Eq. (A11) and Eq. (A12) into Eq. (D2) gives

$$T(N, q, x) \sim \frac{\ln N}{2 \left[ q \frac{3-2x}{1-x} - (1-q)\mathcal{A}_1(x) \right]}, \quad (\text{D6})$$

in agreement with Eq. (30) in the main text. Equivalently, in terms of the dimensionless distance from threshold  $\kappa > 1$ ,

$$\begin{aligned} T(N, \kappa, x) &\sim \frac{\ln N}{2(\kappa - 1)\mathcal{A}_1(x)} \\ &= \frac{\ln N}{(\kappa - 1)(1-x) \sum_{n \geq 3} x^{n-3} 2^{3-n} S_n}, \end{aligned} \quad (\text{D7})$$

### 3. Truncated power-law distribution

Consider the annealed power-law ensemble  $P(n) = n^{-\alpha}/Z_N(\alpha)$  with a hard cutoff  $n_{\max} = N$  and exponent  $\alpha > 0$ . Using  $\langle n \rangle = B_N(\alpha)/Z_N(\alpha)$  and  $\mathcal{A}_1(\alpha) = C_N(\alpha)/(2Z_N(\alpha))$  (with  $Z_N$ ,  $B_N$ , and  $C_N$  defined in Sec. B 1c), Eq. (D2) yields

$$\mathcal{B}(q, \alpha; N) = \frac{Z_N(\alpha)}{2q B_N(\alpha) - (1-q) C_N(\alpha)}. \quad (\text{D8})$$

Importantly, the disordering-time analysis requires the stability condition  $\lambda_N > 0$ , i.e.,

$$2q B_N(\alpha) - (1-q) C_N(\alpha) > 0, \quad (\text{D9})$$

which is equivalent to  $q > q_c(N)$  with

$$q_c(N) = \frac{C_N(\alpha)}{C_N(\alpha) + 2B_N(\alpha)}. \quad (\text{D10})$$

For  $\alpha \leq 5/2$ ,  $C_N(\alpha)$  diverges with  $N$  while  $B_N(\alpha)$  grows more slowly (or converges), implying  $q_c(N) \rightarrow 1$ . Therefore, at fixed absolute  $q < 1$  the inequality (D9) eventually fails and the mixed fixed point becomes unstable; in that case the MFPT to reach the neighborhood of  $c = 1/2$  is not the relevant large- $N$  descriptor. In finite systems one may still enforce the disordered regime by choosing  $q > q_c(N)$ , and then Eqs. (D2) and (D8) remain valid with the  $N$ -dependent  $\mathcal{B}(q, \alpha; N)$ .

For  $\alpha > 5/2$ , all three sums converge to finite constants:  $Z_N \rightarrow \zeta(\alpha, 3)$ ,  $B_N \rightarrow \zeta(\alpha - 1, 3)$ , and  $C_N \rightarrow C^{(\infty)}(\alpha) \equiv \sum_{n=3}^{\infty} n^{-\alpha} 2^{3-n} S_n$ . The prefactor thus becomes independent of  $N$ :

$$\mathcal{B}(q, \alpha) = \frac{\zeta(\alpha, 3)}{2q\zeta(\alpha - 1, 3) - (1-q)C^{(\infty)}(\alpha)}. \quad (\text{D11})$$

Using the parameterization  $q = \kappa q_c(\alpha)$  with  $\kappa > 1$  (well-defined only when  $q_c(\alpha) < 1$ , i.e. for  $\alpha > 5/2$ ), Eq. (D11) simplifies to

$$\mathcal{B}(\kappa, \alpha) = \frac{\zeta(\alpha, 3)}{(\kappa - 1)C^{(\infty)}(\alpha)}. \quad (\text{D12})$$

Thus, we recover the logarithmic scaling  $T_{\text{dis}} \sim \mathcal{B} \ln N$  in this regime.

This result corresponds to the main-text discussion around Eqs. (31)–(32) and the scaling form (33).

### Appendix E: Exit probability for $q = 0$

In the pure majority-rule regime, where  $q = 0$ , the dynamics is up-down symmetric and  $c = 1/2$  is a fixed point. The standard quadrature solution for the exit probability  $E(c)$ , satisfying the backward FP equation as in Eq. (34) is given by

$$E(c_0) = \frac{\int_0^{c_0} \exp \left[ - \int_{1/2}^y \frac{2v(u)}{D(u)} du \right] dy}{\int_0^1 \exp \left[ - \int_{1/2}^y \frac{2v(u)}{D(u)} du \right] dy}, \quad (\text{E1})$$

where the inner integral defines the “potential”  $\Phi(y) \equiv \int_{1/2}^y [2v(u)/D(u)] du$ .

We evaluate the transport coefficients near the symmetric point. For the diffusion coefficient, we use Eq. (4) with  $v(1/2) = 0$  and  $S(c)$  from Eqs. (8) and (9) at  $q = 0$ . This yields

$$D_0(P) \equiv D(1/2) = \frac{1}{N} \sum_{n \geq 3} P(n) K_n, \quad (\text{E2})$$

where  $K_n \equiv S_n^{\text{MR}}(1/2)$  is the second jump moment at the symmetric point:

$$K_n = 2^{-n} \left[ \sum_{\ell > n/2} (n - \ell)^2 \binom{n}{\ell} + \sum_{\ell < n/2} \ell^2 \binom{n}{\ell} \right]. \quad (\text{E3})$$

Substituting the linear drift  $v(c) \simeq \mathcal{A}_1(P)(c - 1/2)$  and the constant diffusion  $D_0(P)$  into the potential yields the harmonic approximation

$$\begin{aligned} \Phi(y) &\simeq \frac{2\mathcal{A}_1(P)}{D_0(P)} \int_{1/2}^y (u - 1/2) du \\ &= \gamma(P) (y - 1/2)^2, \end{aligned} \quad (\text{E4})$$

where  $\gamma(P) \equiv \mathcal{A}_1(P)/D_0(P)$ . Evaluating Eq. (E1) with

this kernel leads to the error-function profile

$$\begin{aligned} E(c_0) &\approx \frac{\int_{-\infty}^{c_0-1/2} \exp[-\gamma(P)s^2] ds}{\int_{-\infty}^{+\infty} \exp[-\gamma(P)s^2] ds} \\ &= \frac{1}{2} \left[ 1 + \text{erf} \left( \sqrt{\gamma(P)} (c_0 - 1/2) \right) \right]. \end{aligned} \quad (\text{E5})$$

The explicit form of  $\gamma(P)$  for the  $n$ -uniform ensemble is

$$\gamma_u(n) = N \frac{2^{2-n} S_n}{K_n}. \quad (\text{E6})$$

For the shifted geometric distribution,  $\gamma(P)$  reads

$$\gamma_g(x) = N \frac{\sum_{n=3}^{\infty} x^{n-3} 2^{2-n} S_n}{\sum_{n=3}^{\infty} x^{n-3} K_n}. \quad (\text{E7})$$

Finally, for the truncated power-law distribution,  $\gamma(P)$  is given by

$$\gamma_{\text{pl}}(N, \alpha) = N \frac{\sum_{n=3}^N n^{-\alpha} 2^{2-n} S_n}{\sum_{n=3}^N n^{-\alpha} K_n}. \quad (\text{E8})$$

---

[1] C. Castellano, S. Fortunato, and V. Loreto, *Rev. Mod. Phys.* **81**, 591 (2009).

[2] T. M. Liggett, *Stochastic interacting systems: contact, voter and exclusion processes*, Vol. 324 (Springer, 2013).

[3] S. Galam, *Sociophysics: A Physicist’s Modeling of Psycho-political Phenomena* (Springer-Verlag, New York, 2012).

[4] S. Galam, *J. Math. Psychol.* **30**, 426 (1986).

[5] S. Galam, *Int. J. Mod. Phys. C* **19**, 409 (2008).

[6] T. Cheon and S. Galam, *Phys. Lett. A* **382**, 1509 (2018).

[7] P. L. Krapivsky and S. Redner, *Phys. Rev. Lett.* **90**, 238701 (2003).

[8] P. Chen and S. Redner, *Phys. Rev. E* **71**, 036101 (2005).

[9] R. Lambiotte, M. Ausloos, and J. Holyst, *Phys. Rev. E* **75**, 030101 (2007).

[10] V. X. Nguyen, G. Xiao, X.-J. Xu, Q. Wu, and C.-Y. Xia, *Sci. Rep.* **10**, 456 (2020).

[11] D. A. Mulya and R. Muslim, *Int. J. Mod. Phys. C* **35**, 2450125 (2024).

[12] R. Muslim, D. A. Mulya, Z. Akbar, and R. A. Nqz, *Chaos Solitons Fractals* **189**, 115718 (2024).

[13] A. Azhari and R. Muslim, *Int. J. Mod. Phys. C* **34**, 2350088 (2023).

[14] N. Crokidakis and P. M. C. de Oliveira, *Phys. Rev. E* **92**, 062122 (2015).

[15] R. Muslim, S. A. Wella, and A. R. Nugraha, *Physica A* **608**, 128307 (2022).

[16] A. L. Oestereich, M. A. Pires, S. M. Duarte Queirós, and N. Crokidakis, *Physics* **5**, 911 (2023).

[17] F. Battiston, G. Cencetti, I. Iacopini, V. Latora, M. Lucas, A. Patania, J.-G. Young, and G. Petri, *Phys. Rep.* **874**, 1 (2020).

[18] S. Boccaletti, P. De Lellis, C. Del Genio, K. Alfaro-Bittner, R. Criado, S. Jalan, and M. Romance, *Phys. Rep.* **1018**, 1 (2023).

[19] C. Bick, E. Gross, H. A. Harrington, and M. T. Schaub, *SIAM Rev.* **65**, 686 (2023).

[20] I. Iacopini, G. Petri, A. Barrat, and V. Latora, *Nat. Commun.* **10**, 2485 (2019).

[21] G. F. de Arruda, G. Petri, and Y. Moreno, *Phys. Rev. Res.* **2**, 023032 (2020).

[22] P. S. Skardal and A. Arenas, *Commun. Phys.* **3**, 218 (2020).

[23] A. P. Millán, J. J. Torres, and G. Bianconi, *Phys. Rev. Lett.* **124**, 218301 (2020).

[24] Y. Zhang, M. Lucas, and F. Battiston, *Nat. Commun.* **14**, 1605 (2023).

[25] S. Majhi, M. Perc, and D. Ghosh, *J. R. Soc. Interface* **19**, 20220043 (2022).

[26] J. Stehlé, N. Voirin, A. Barrat, C. Cattuto, L. Isella, J.-F. Pinton, M. Quaggiotto, W. Van den Broeck, C. Régis, B. Lina, *et al.*, *PLoS One* **6**, e23176 (2011).

[27] R. Mastrandrea, J. Fournet, and A. Barrat, *PLoS One* **10**, e0136497 (2015).

[28] A. Patania, G. Petri, and F. Vaccarino, *EPJ Data Sci.* **6**, 1 (2017).

[29] A. R. Benson, D. F. Gleich, and J. Leskovec, *Science* **353**, 163 (2016).

[30] A. R. Benson, R. Abebe, M. T. Schaub, A. Jadbabaie, and J. Kleinberg, *Proc. Natl. Acad. Sci. U.S.A.* **115**, E11221 (2018).

[31] D. Roh and K.-I. Goh, *J. Korean Phys. Soc.* **83**, 713

(2023).

[32] E. Bakshy, S. Messing, and L. A. Adamic, *Science* **348**, 1130 (2015).

[33] A. Abramiuk-Szurlej, M. Szurlej, and K. Sznajd-Weron, *Rigorous agent-based modeling is critical: Modeling the diffusion of green products and practices*, Tech. Rep. (Department of Operations Research and Business Intelligence, Wroclaw . . ., 2023).

[34] J. Noonan and R. Lambiotte, *Phys. Rev. E* **104**, 024316 (2021).

[35] N. Lanchier and J. Neufer, *J. Stat. Phys.* **151**, 21 (2013).

[36] L. Neuhäuser, R. Lambiotte, and M. T. Schaub, in *Higher-Order Systems* (Springer, 2022) pp. 347–376.

[37] R. Pastor-Satorras, C. Castellano, P. Van Mieghem, and A. Vespignani, *Rev. Mod. Phys.* **87**, 925 (2015).

[38] J. P. Gleeson, *Phys. Rev. X* **3**, 021004 (2013).

[39] S. E. Asch, in *Organizational influence processes* (Routledge, 2016) pp. 295–303.

[40] H. Mercier and O. Morin, *Evol. Hum. Sci.* **1**, e6 (2019).

[41] A. T. Hartnett, E. Schertzer, S. A. Levin, and I. D. Couzin, *Phys. Rev. Lett.* **116**, 038701 (2016).

[42] M. J. de Oliveira, *J. Stat. Phys.* **66**, 273 (1992).

[43] H. Chen, C. Shen, G. He, H. Zhang, and Z. Hou, *Phys. Rev. E* **91**, 022816 (2015).

[44] H. Chen, S. Wang, C. Shen, H. Zhang, and G. Bianconi, *Phys. Rev. E* **102**, 062311 (2020).

[45] R. Muslim, J. Kim, N. Oikawa, A. R. NQZ, and Z. Akbar, *Phys. Rev. E* **112**, 034312 (2025).

[46] F. L. Forgerini, N. Crokidakis, and M. A. Carvalho, *Int. J. Mod. Phys. C* , 2450082 (2024).

[47] C. W. Gardiner, Springer Ser. Synerg. (1985).

[48] N. G. Van Kampen, *Stochastic processes in physics and chemistry*, Vol. 1 (Elsevier, 1992).

[49] A. Carro, R. Toral, and M. San Miguel, *Sci. Rep.* **6**, 24775 (2016).

[50] R. Muslim, R. A. Nqz, and M. A. Khalif, *Physica A* **633**, 129358 (2024).